AIP Advances

The influence of temperature on the electrical conductivity of GaN piezoelectric semiconductors

Cite as: AIP Advances **13**, 015105 (2023); https://doi.org/10.1063/5.0133129
Submitted: 04 November 2022 • Accepted: 11 December 2022 • Published Online: 04 January 2023

YanPeng Qiao, MingHao Zhao, GuoShuai Qin, et al.

The influence of temperature on the electrical conductivity of GaN piezoelectric semiconductors

Cite as: AIP Advances 13, 015105 (2023); doi: 10.1063/5.0133129
Submitted: 4 November 2022 • Accepted: 11 December 2022 •
Published Online: 4 January 2023

YanPeng Qiao,[1] MingHao Zhao,[1] GuoShuai Qin,[2] Chunsheng Lu,[3] and CuiYing Fan[1,a)]

AFFILIATIONS

[1] School of Mechanics and Safety Engineering, Zhengzhou University, No. 100 Science Road, Henan Province, Zhengzhou 450001, China
[2] School of Electromechanical Engineering, Henan University of Technology, Henan, Zhengzhou 450001, China
[3] School of Civil and Mechanical Engineering, Curtin University, Western Australia, Perth 6845, Australia

[a)] **Author to whom correspondence should be addressed:** fancy@zzu.edu.cn

ABSTRACT

GaN is an excellent material choice for power devices due to its excellent properties such as super wide bandgap width and high electron mobility. However, the problem of temperature affects the thermo reliability and hinders the potential of GaN devices. In this paper, the electrical properties of GaN under temperature have been studied by the combination of numerical simulation and experimental research. The electric current change and electrical resistivity of polarized and depolarized GaN semiconductor samples were tested in an environment-test cabinet. Based on the influence of temperature, the expression of the resistivity curve vs temperature was established for polarized and depolarized GaN samples. It is shown that the resistivity model predictions are consistent with experimental results. The I–V characteristic curves under different temperatures were also measured. Thus, such a model is instructive to the reliable design of GaN high-temperature devices. The findings will be instructive to the optimal design of GaN electronic components.

I. INTRODUCTION

Because of their excellent piezoelectric and semiconductor properties, piezoelectric semiconductor materials have been widely used in electronic components,[1] such as biosensors,[2] resonators,[3–5] and piezoresistive sensors[6,7] and other equipment. These electronic components need to inevitably work under different temperature environments.[8] However, semiconductor devices are sensitive to temperature, which affects the distribution of carriers and electrical current transport capacity.[9–12] Meanwhile, resistance and current have a great influence on the sensitivity of an electronic components.[13,14] The existing results show a nonlinear variation in resistivity with temperature.[15,16] In applications, the GaN piezoelectric semiconductor with a wide bandgap is usually applied to develop new semiconductor materials for radio frequency components, high-electron-mobility transistors, broadband communication, and microelectronic and optoelectronic devices. Meanwhile, GaN piezoelectric semiconductors exhibit thermoelectric, pyroelectric, and piezoelectric coupling characteristics. Therefore, it is of great practical significance to investigate the performance of GaN piezoelectric semiconductors under different temperatures.

Recently, most of the research on piezoelectric semiconductor under a temperature load remains in the theoretical and numerical stage, insomuch that their governing equations and boundary conditions are complex and nonlinear, while these studies normally adopted the linear based equation.[17–20] However, linearization can only be applied in the case of relatively small carrier fluctuation. Taking the nonlinear features of governing equations into account, the corresponding resistance was assumed to be a constant value under different temperatures.[21] To the best of our knowledge, there are only a few experiments on semiconductors subjected to temperature, such as those determining the electrical characteristics of a Si/Al semiconductor structure at low temperatures[22] and the I–V characteristic curves of a ZnO Schottky junction,[23,24] as well

as heterostructures of AlGaN and bending strength of GaN.[25] As present, comprehensive studies on the electrical properties under different thermal environments are lacking, especially for semiconductors with piezoelectric properties, which are insufficient to meet the needs of design of GaN semiconductor devices.

In order to accurately scrutinize these electron devices, it is urgent to understand the influence of temperature on the electric performance of piezoelectric semiconductors from the experimental point of view. In this paper, GaN ceramics, a typical kind of piezoelectric semiconductors, are investigated by using experimental tests and numerical simulations. The results will highlight the influence of temperature on the resistivity, current, and I–V characteristic of piezoelectric semiconductors. It is also expected that the findings can provide a reference for the optimal design and application of piezoelectric semiconductor electron devices.

II. COUPLING THEORY FOR A PIEZOELECTRIC SEMICONDUCTOR

Since GaN used here is a typical n-type semiconductor, its electron concentration is much higher than the hole concentration, that is, the impact of a hole can be ignored in the calculation process. As a wide-bandgap semiconductor with a rather high ionization degree, it can be assumed to be completely ionized. At the same time, the influence of carrier recombination is small under non-specific conditions, which can be approximately ignored. Therefore, for such a three-dimensional piezoelectric semiconductor dynamic problem, according to the principles of force balance, charge conservation, current continuity, and heat balance in the $Ox_1x_2x_3$ coordinate system (see Fig. 1), the simplified equilibrium equations can be written as

$$\begin{aligned} \sigma_{ij,j} &= \rho_m \ddot{u}_i, \\ D_{i,i} &= q(N_D - n), \\ J_{i,i} &= q\dot{n}, \\ h_{i,i} &= J_i E_i, \end{aligned} \tag{1}$$

where σ_{ij} is the stress tensor, ρ_m is the mass density, u_i is the displacement vector, D_i is the electric displacement vector, q is the electronic charge ($q = 1.602 \times 10^{-19}$ C), N_D is the donor concentration ($N_D = 1.29 \times 10^{23}$ m^{-3}), n is the concentration of electrons, J_i is the electron current density, h_i is heat flux density, and E_i is the electric field intensity.

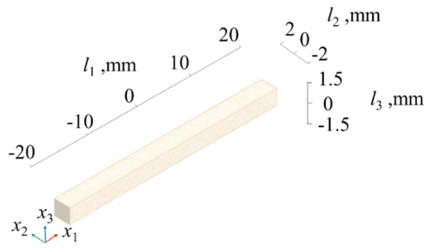

FIG. 1. Illustrative diagram of a three-dimensional piezoelectric semiconductor in a coordinate system.

For the piezoelectric semiconductor polarized along the z (or thickness) direction, three-dimensional constitutive equations for the n-type piezoelectric semiconductor can be represented as

$$\begin{aligned} \sigma_{ij} &= c^{\mathrm{E}}_{ijks}\varepsilon_{ks} - e_{kij}E_k - \lambda_{ij}(T - T_0), \\ D_i &= \kappa_{ij}E_j + e_{kij}\varepsilon_{jk} + p(T - T_0), \\ J_i &= qn\mu_{ij}E_j + qd_{ij}n_{,j} - qn\mu_{ij}S_m T_{,j}, \\ h_i &= -k_{ij}T_{,i} \quad (i,j,k,\ s = 1,2,3), \end{aligned} \tag{2}$$

where c^{E}_{ijks}, e_{kij}, and κ_{ij} are the elastic coefficient, piezoelectric constant, and relative dielectric constant, respectively; λ_{ij}, p, and S_m are the thermal expansion, pyroelectric, and Seebeck coefficients, respectively; k_{ij} is the thermal conductivity; μ_{ij} and d_{ij} are the carrier mobility and diffusion constants, respectively; ε_{ks} is the strain tensor; T is the absolute temperature; and T_0 is the reference temperature. The geometric equations are

$$\begin{aligned} \varepsilon_{ij} &= \frac{1}{2}(u_{i,j} + u_{j,i}), \\ E_i &= -\varphi_{,i}, \end{aligned} \tag{3}$$

where φ is the electric potential.

III. EXPERIMENTAL CONDITIONS

The sample size of GaN was determined according to the test standard.[26] As illustrated in Fig. 1, the samples with length l_1 = 40.0 mm, width l_2 = 4.0 mm, and thickness l_3 = 3.0 mm were prepared for temperature dependent testing. A special interlayer polarized method[27] as shown in Fig. 2 was used to polarize one-half of the samples along their thickness directions. According to the voltage divider, a DC voltage of 21 kV was applied to both ends of an electrode. To avoid discharging, the samples were polarized in silicone oil under a field intensity of 24 kV cm^{-1} for 40 min, which is almost three times the coercive field of GaN piezoelectric semiconductors (8.19 kV cm^{-1}). The other half of the samples were depolarized by baking at 525 K (with a Curie point of 490 K) for 30 min.[28] The corresponding material constants are listed in Table I.

The temperature dependent tests were carried out in an environmental cabinet with constant power, as illustrated in Fig. 3. Silver

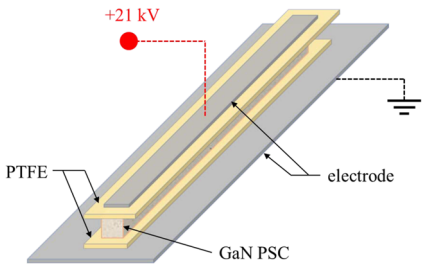

FIG. 2. Schematic diagram of a high-voltage interlayer polarization jig, where PSC and PTFE indicate the piezoelectric semiconductor and polytetrafluoroethylene, respectively.

TABLE I. The relevant material constants of GaN under 300 K.[a]

Property	Unit	Parameters		
Elastic coefficient $\boldsymbol{c}$	GPa	$c_{11} = 298.4$	$c_{12} = 121.0$	$c_{13} = 145.2$
		$c_{33} = 289.2$	$c_{44} = 23.1$	
Piezoelectric constant $\boldsymbol{e}$	C/m^2	$e_{15} = -0.31$	$e_{31} = -0.52$	$e_{33} = 0.61$
Relative dielectric constant $\boldsymbol{\kappa}$	C/V m	$\kappa_{11} = 9.6\kappa_0$	$\kappa_{33} = 10.3\kappa_0$	$\kappa_0 = 8.854 \times 10^{-12}$
Electron mobility $\boldsymbol{\mu}$	cm^2/V s	$\mu_{11} = 653$	$\mu_{33} = 982$	
Diffusion coefficient $\boldsymbol{d}$	cm^2/s	$d_{11} = 16.99$	$d_{33} = 25.53$	
Heat transfer coefficient $\boldsymbol{k}$	W/mK	$k_{11} = 0.633$	$k_{33} = 0.548$	
Thermal expansion coefficient $\boldsymbol{\lambda}$	Pa/K	$\lambda_{11} = 35\,737$	$\lambda_{33} = 29\,666$	
Pyroelectric coefficient $\boldsymbol{p}$	C/Km	$p = -3 \times 10^{-6}$		
Seebeck coefficient $\boldsymbol{S_m}$	V/K	$S_m = 8.2 \times 10^{-5}$		

[a]Here, $c_{\gamma\eta} = c^{E}_{ijks}$, $e_{kij} = e_{k\gamma}$, and the subscripts γ and η are from 1 to 6.

paste was plated on the both ends of the sample as an electrode, and sliver wire (with a diameter of 0.2 mm) was welded to the electrode in order to connect with the measuring instrument.

To solve the governing equations of a three-dimensional GaN piezoelectric semiconductor with x_3-polarization as listed in Sec. II, the boundary conditions are as follows:

(1) The displacement boundary conditions are

$$u_1 = 0, \quad u_2 = 0, \quad u_3 = 0, \quad \text{at } x_1 = -15 \text{ mm}, \quad x_3 = -1.5 \text{ mm},$$
$$u_2 = 0, \quad u_3 = 0, \quad \text{at } x_1 = 15 \text{ mm}, \quad x_3 = -1.5 \text{ mm}. \tag{4}$$

(2) The electric boundary conditions at the silver electrodes and GaN contact for Schottky[29] are

$$\varphi = 0, \quad J_1 \cdot l = -qv_{res}(n - n_m), \quad \text{at } x_1 = -20 \text{ mm},$$
$$\varphi = \varphi_0, \quad J_1 \cdot l = -qv_{res}(n - n_m), \quad \text{at } x_1 = 20 \text{ mm}, \tag{5}$$

where v_{res} is the thermal recombination rate of electrons at the Schottky contact ($v_{\text{res}} = 60\ 154$ m/s), n_m is the critical electron concentration ($n_m = 4.58 \times 10^{21}$ m^{-3}), and l is the direction vector. φ_0 is the value of the applied electric potential.

(3) The thermal boundary condition is

$$T = f(t), \quad \text{at } x_1 = \pm 20 \text{ mm}, \quad x_2 = \pm 2 \text{ mm}, \quad x_3 = \pm 1.5 \text{ mm}, \tag{6}$$

where $f(t)$ is the temperature change function of time t in the environment cabinet.

The heat conduction equation is used to determine the time required for a sample to reach the thermal equilibrium,[30] that is,

$$\rho_m C_p \frac{\partial T}{\partial t} + K_m \nabla^2 T = Q, \tag{7}$$

where C_p is the thermal capacity [$C_p = 623$ J(kg K)$^{-1}$], K_m is the heat transfer coefficient [$K_m = 0.633$ W(m K)$^{-1}$], ∇ is the Hamiltonian operator, and Q is the heat. For one target temperature, the times to reach thermal equilibrium are the same for polarized and depolarized GaN samples, as shown in Fig. 4. It implies that the GaN sample takes about 200 s to be basically stable under different target temperatures. Therefore, during the following experiment, the experiment result is obtained after maintaining the warmth for 200 s.

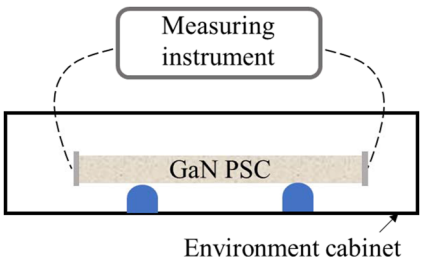

FIG. 3. Illustrative configuration of the temperature dependent experiment.

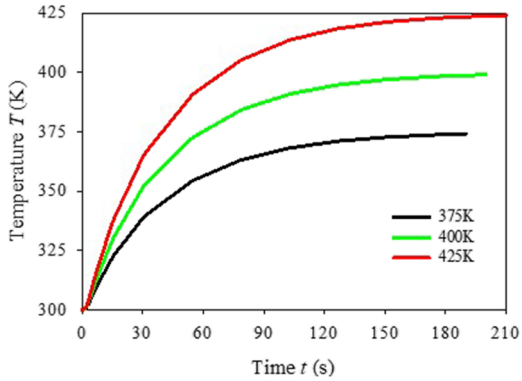

FIG. 4. Time required to reach thermal equilibrium in a GaN sample under different target temperatures.

IV. EXPERIMENT RESULTS AND DISCUSSION

For the depolarized GaN samples without voltage($\varphi_0 = 0$), the currents under different setting temperatures are shown in Fig. 5. It is seen that the current gradually decreases with the increase in temperature and finally tends to be stable at 390 K. The temperature affects the movement of free electrons, but after 390 K, free electrons reach an equilibrium state. Meanwhile, the stable current for low temperature is bigger than that for high temperature. The corresponding polarized GaN samples have similar curves of current with temperature (see Fig. 5); after 390 K, the current also tends to be stable. However, the current for polarized GaN is bigger than that of depolarized GaN under the same temperature, and this phenomenon is similar to other GaN experimental results where the polarization increases the transport capacity of current.[28]

In order to explain the variation in electrical conductivity, the resistivity of polarized GaN and depolarized GaN is measured with the change in temperature, as shown in Fig. 6. The resistivity trend with the change in temperature is consistent with most of the semiconductor containing impurities. The resistivity for both polarization and depolarization increases gradually from room temperature to 390 K and then decreases after 390 K. Based on the existing semiconductor knowledge, these changed resistivities of GaN have the following physical phenomena:

(1) When the temperature is low, the impurity is completely ionized. As the temperature increases from room temperature, the intrinsic excitation is not significant, so the carrier concentration does not change with temperature.
(2) Then, since lattice vibration scattering becomes the main contradiction, the electron mobility decreases with the increase in temperature. Hence, the resistivity increases with the increase in temperature.
(3) As the temperature continues to increase, the intrinsic excitation increases rapidly, and generation of a large number of intrinsic carriers outweighs the effect of reduced mobility on resistivity. Then, the intrinsic excitation becomes the main aspect of contradiction, and the resistivity of impurity semiconductors decreases sharply with the increase in temperature.

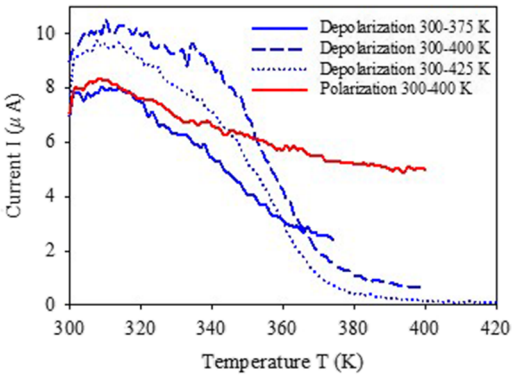

FIG. 5. Current in polarized and depolarized GaN samples vs temperature changing from room to different target temperatures.

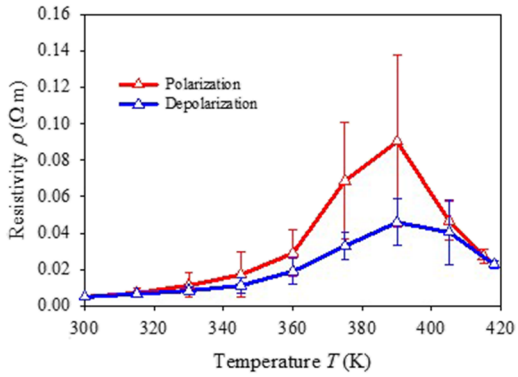

FIG. 6. Tested resistivity with error bars vs temperature.

(4) It is seen that the change in resistivity is consistent with current in Fig. 5. As the temperature increases from 340 to 390 K, the resistivity increases rapidly, and the current decreases. After 390 K, although the resistivity decreases, the current does not decrease but remains to be constant. This is attributed to the recombination of ionized free electrons that are accelerated with the increase in temperature and the appearance of non-electric properties.

Based on existing semiconductor knowledge, the resistivity ρ depends on carrier concentration n and electron mobility μ for the n-type semiconductor,[15]

$$\rho = \frac{1}{nq\mu}, \tag{8}$$

where for the high purity of GaN ($N_D = 1.29 \times 10^{23}$ m^{-3}), the influence of temperature on the carrier concentration and electron mobility can be expressed as

$$n = 4.82 \times 10^{15}\left(\frac{m_p^* m_n^*}{m_0^2}\right)^{3/4} T^{1.5} e^{\left(-\frac{E_g}{2k_0 T}\right)}, \qquad \mu = \frac{q}{m^*}\frac{1}{AT^{1.5}}, \tag{9}$$

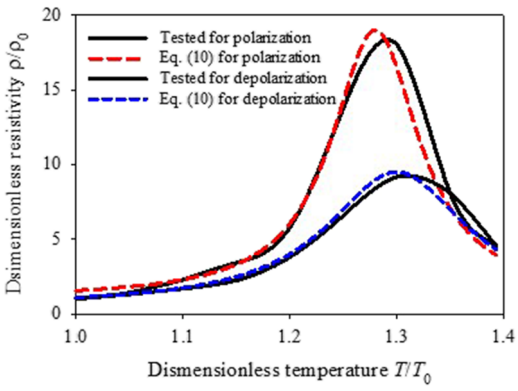

FIG. 7. Comparison diagram of resistivity between tested results and Eq. (10).

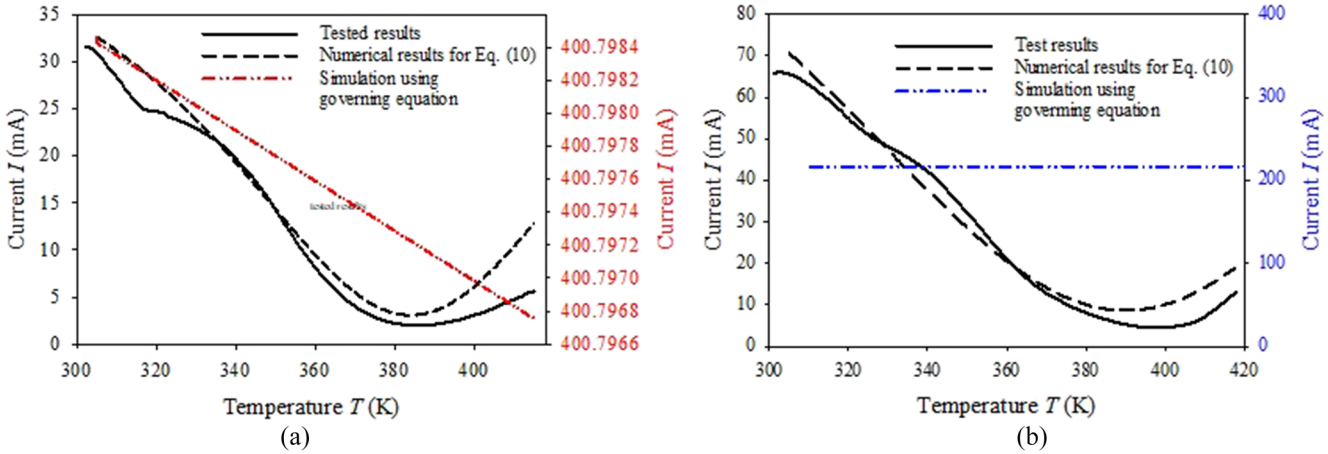

FIG. 8. Comparison of the current vs temperature in (a) polarized and (b) depolarized samples, where the left axis is the experiment and fitting and the right side is the simulation.

where m_p^*, m_n^*, m, and m^* are the corresponding mass constants and E_g and k_0 are the corresponding material constants. Therefore, the resistivity only depends on the temperature T. Based on the variation tendency of resistivity for GaN and the expression of resistivity for metallic glasses and the Ni–Cr alloy,[31,32] the relevant resistivities can be fitted well by the following functions based on the test results and Eqs. (8) and (9):

$$\rho = \rho_0(1 + f(T)), \tag{10}$$

where $\rho_0 = 5 \times 10^{-3}$ Ω m for the reference temperature at $T_0 = 300$ K and

$$f(T) = \frac{18}{1 + \left(20\frac{T}{T_0} - 25.6\right)^2}, \quad \text{for polarized GaN,} \tag{11a}$$

$$f(T) = \frac{18}{1 + \left(12.5\frac{T}{T_0} - 16.25\right)^2}, \quad \text{for depolarized GaN.} \tag{11b}$$

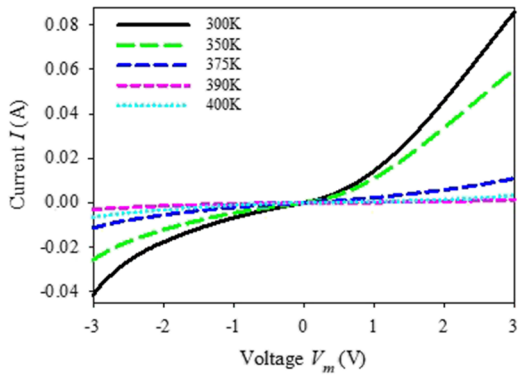

FIG. 9. I–V characteristic curves at different experimental temperatures.

It can be seen from Fig. 7 that the resistivity functions in Eq. (10) can be fitted well with the tested results for the poling direction along the thickness direction. In the poling direction along the length direction (x_1-direction), the current transport performance has a little change in the poling direction ones with depolarization,[27] and the corresponding resistivity functions are similar to Eqs. (10) and (11b). Therefore, Eq. (10) can describe the resistivities of polarized and depolarized GaN.

To study the electrical conductivity under voltage, 1 V voltage ($\varphi_0 = 1$ V) was applied to both ends of a sample to measure its current. Then, the resistivity in Eq. (10) was input into COMSOL to obtain the fitting current change diagram. As shown in Fig. 8(a) for polarized samples, it is obvious that the numerical results obtained using Eqs. (10) and (11a) are in good agreement with the tested results. However, the numerical results of current using constant resistivity are almost constant; meanwhile, it is much bigger than the experimental ones. Similarly, as seen in Fig. 8(b), the currents for depolarized GaN from Eqs. (10) and (11b) are also consistent with the tested results, that is, there is a big gap between the experimental results and those obtained by the governing equation.

Finally, we tested the I–V characteristic curve of a piezoelectric semiconductor sample under different temperatures, as shown in Fig. 9. It can be seen that the higher the temperature is, the less obvious the I–V characteristic curve will be. However, after 390 K, the variation trend is opposite. This phenomenon is consistent with the resistivity variation trend in Eq. (10) and Fig. 6.

V. CONCLUSIONS

In this paper, we have experimentally measured the influence of temperature on the current and resistivity of GaN samples, as well as the I–V characteristic curves under different temperatures. The expressions of resistivity vs temperature have been obtained for polarized and depolarized GaN. The numerical results based on the resistivity curves are consistent with the experimental tested results.

Then, the corresponding I–V characteristic curves at different temperatures once again illustrate the resistivity variation. The influence of temperature on the electrical conductivity of GaN piezoelectric semiconductors is especially obvious, where the maximum resistance is achieved at around 390 K. Finally, the regulation mechanism of temperature on the electrical conductivity of GaN is given. This will be instructive to the design of GaN devices, especially the ones related to temperature.

ACKNOWLEDGMENTS

This work has been supported by the National Natural Science Foundation of China (Grant Nos. 12002316 and 12272353).

AUTHOR DECLARATIONS

Conflict of Interest

The authors have no conflicts to disclose.

Author Contributions

YanPeng Qiao: Writing – original draft (equal). **MingHao Zhao**: Funding acquisition (equal); Investigation (equal). **GuoShuai Qin**: Data curation (equal). **Chunsheng Lu**: Writing – review & editing (equal). **CuiYing Fan**: Project administration (equal); Writing – original draft (equal); Writing – review & editing (equal).

DATA AVAILABILITY

The data that support the findings of this study are available from the corresponding author upon reasonable request.

REFERENCES

[1]M. A. Fraga, H. Furlan, R. S. Pessoa, and M. Massi, Microsyst. Technol. **20**, 9 (2014).
[2]A. Fulati, S. Usman Ali, M. Riaz, G. Amin, O. Nur, and M. Willander, Sensors **9**, 8911 (2009).
[3]D. Chen, J. J. Wang, Q. X. Liu, Y. Xu, D. H. Li, and Y. J. Li, J. Micromech. Microeng. **21**, 115018 (2011).
[4]Z. Wang, X. Qiu, S. J. Chen, W. Pang, H. Zhang, J. Shi, and H. Yu, Thin Solid Films **519**, 6144 (2011).
[5]D. Chen, Z. Zhang, J. Ma, and W. Wang, Sensors **17**, 1015 (2017).
[6]J. K. Luo, Y. Q. Fu, H. R. Le, J. A. Williams, S. M. Spearing, and W. I. Milne, J. Micromech. Microeng. **17**, S147 (2007).
[7]Z. Cao; V. Mike, and A. Dean, in *2010 IEEE 23rd International Conference on Micro Electro Mechanical Systems (MEMS)* (IEEE, 2010), Vol. 51.
[8]J. Chen and X. Zhang, J. Mater. Sci. **54**, 2392 (2018).
[9]M. H. Zhao, C. H. Yang, C. Y. Fan, and Q. Y. Zhang, Z. Angew. Math. Mech. **100**, e201900302 (2020).
[10]Z. Yang, L. Sun, C. Zhang, C. Zhang, and C. Gao, Mech. Mater. **164**, 104153 (2022).
[11]R. Cheng, C. Zhang, and J. Yang, J. Electron. Mater. **48**, 4939 (2019).
[12]Y. Qu, F. Jin, and J. Yang, J. Appl. Phys. **131**, 094502 (2022).
[13]N. S. Ali, *A Multifunctional MEMS Pressure and Temperature Sensor for Harsh Environment Applications* (University of Waterloo UWSpace, University of Waterloo, 2013).
[14]L. Kang, Y. Shi, J. Zhang, C. Huang, N. Zhang, Y. He, W. Li, C. Wang, X. Wu, and X. Zhou, Microelectron. Eng. **216**, 111052 (2019).
[15]E. K. Liu, B. S. Zhu, and J. S. Luo, *The Physics of Semiconductors* (Publishing House of Electronics Industry, 2017), ISBN: 978-7-121-32007-1.
[16]M. Rahmani, C. Pithan, and R. Waser, J. Eur. Ceram. Soc. **39**, 4800 (2019).
[17]A. R. Hutson and D. L. White, J. Appl. Phys. **33**, 40 (1962).
[18]J. Sladek, V. Sladek, E. Pan, and M. Wünsche, Eng. Fract. Mech. **126**, 27 (2014).
[19]X. Dai, F. Zhu, Z. Qian, and J. Yang, Nano Energy **43**, 22 (2018).
[20]R. Cheng, C. Zhang, W. Chen, and J. Yang, Nano Energy **66**, 104081 (2019).
[21]M. Guo, C. Lu, G. Qin, and M. Zhao, J. Electron. Mater. **50**, 947 (2021).
[22]K. Şükrü, C. Muzaffer, and T. Abdülmecit, Mater. Sci. Semicond. Process. **28**, 135 (2014).
[23]M. W. Allen, R. J. Mendelsberg, R. J. Reeves, and S. M. Durbin, Appl. Phys. Lett. **94**, 103508 (2009).
[24]K. Ahmeda, B. Ubochi, B. Benbakhti, S. J. Duffy, A. Soltani, W. D. Zhang, and K. Kalna, in *2017 IEEE Translations and Content Mining are Permitted for Academic Research only* (IEEE, 2017), p. 20946.
[25]M. Zhao, Y. Wang, C. Guo, C. Lu, G. Xu, and G. Qin, Ceram. Int. **48**, 2771 (2022).
[26]ISO 14704, International Organization for Standardization, Geneva, Switzerland, 2016.
[27]G. Qin, C. Lu, M. Umair, and M. Zhao, Ceram. Int. **46**, 5331 (2020).
[28]G. Qin, S. Ma, C. Lu, G. Wang, and M. Zhao, Ceram. Int. **44**, 4169 (2018).
[29]F. R. Pierret, *Semiconductor Device Fundamentals* (Pearson, Indiana, 1996).
[30]Y. R. Li and S. Y. Wu, *Heat Transfer* (Science Press, Beijing, 2012), ISBN: 9787030343178.
[31]N. C. Chuang, J. T. Lin, and H. R. Chen, Vacuum **119**, 200 (2015).
[32]U. Mizutani, M. Tanaka, and H. Sato, J. Phys. F: Met. Phys. **17**, 131 (1987).